



Limb, M. A. L., Suardiaz Del Rio, R., Grant, I. M., & Mulholland, A. (2019). Quantum Mechanics/Molecular Mechanics Simulations Show Saccharide Distortion is Required for Reaction in Hen Egg-White Lysozyme. *Chemistry - A European Journal*, 25(3), 764-768.
<https://doi.org/10.1002/chem.201805250>

Peer reviewed version

Link to published version (if available):
[10.1002/chem.201805250](https://doi.org/10.1002/chem.201805250)

[Link to publication record in Explore Bristol Research](#)
PDF-document

This is the author accepted manuscript (AAM). The final published version (version of record) is available online via Wiley at <https://onlinelibrary.wiley.com/doi/abs/10.1002/chem.201805250> . Please refer to any applicable terms of use of the publisher.

University of Bristol - Explore Bristol Research

General rights

This document is made available in accordance with publisher policies. Please cite only the published version using the reference above. Full terms of use are available:
<http://www.bristol.ac.uk/pure/about/ebr-terms>

QM/MM Simulations Show Saccharide Distortion is Required for Reaction in Hen Egg-White Lysozyme

Michael A. L. Limb,^[a] Reynier Suardíaz,^[a] Ian M. Grant^[b] Adrian J. Mulholland*^[a]

Abstract: Hybrid quantum mechanics / molecular mechanics (QM/MM) calculations on lysozyme show significant distortion of the bound saccharide is required to facilitate the catalytic reaction.

Hen egg-white lysozyme (HEWL) belongs to a large family of enzymes known as the glycoside hydrolases (GH) or glycosidases, whose function is to catalyze the cleavage of glycosidic bonds found in complex carbohydrates.^[1] HEWL is a retaining β -glycosidase and is a mechanistic paradigm as the first enzyme to have its 3D structure solved by X-ray crystallography, as well as the subject of the first ever QM/MM calculation performed on an enzyme.^[2] Critical to understanding catalysis in GHs, and for designing inhibitors for these enzymes, is identifying the conformations adopted by the pyranose ring of carbohydrate substrates during reaction.^[3] The nature of the bound and reactive conformation of the substrate in HEWL and other related enzymes has been a long-standing debate. Here, a combination of molecular mechanics (MM) molecular dynamics (MD) and QM/MM-umbrella sampling and adiabatic mapping simulations on HEWL identify the conformational itinerary over the course of the enzyme-catalysed reaction, including indicating that reaction may occur via nucleophilic attack of the *anti* lone pair of Asp52 and subsequent conformational change. The results demonstrate that saccharide distortion is essential for efficient reaction.

HEWL catalyses the cleavage of a glycosidic bond found in its natural substrate, peptidoglycan, a key component of the cell wall of Gram-negative bacteria, consisting of alternating *N*-acetyl-muramic acid (NAM) and *N*-acetyl-D-glucosamine (NAG) pyranose rings joined by 1,4 β glycosidic bonds. The enzyme binds a six-saccharide section of the polysaccharide chain in six sites in a binding cleft (termed A to F, or -4, to +2).^[4] HEWL catalyses the cleavage of the glycosidic bond between the NAM and NAG rings located in the -1 and +1 binding sites (NAM-D and NAG-E, respectively). The reaction is now believed^[5] to take place via a retaining double-displacement mechanism originally suggested by Koshland, mediated by Glu35 acting as the general acid and Asp52 as the base.^[6] In the first step of the reaction, a proton is transferred from Glu35 onto the oxygen of the glycosidic bond between NAM-D and NAG-E, followed by cleavage of the bond and formation of a covalent intermediate. This intermediate is broken down by attack of a water molecule on the top face of NAM-D at the anomeric carbon, in a SN2-type reaction, with cleavage of the O $\delta_{2\text{Asp52}}$ -C1_{NAM-D} bond formed in the first step. This results in the formation of the product with retention of the stereochemistry of the anomeric carbon. The intermediate is proposed to be flanked by two oxocarbenium ion-like transition states (TSs) with a conformation in which the C5-

O5-C1-C2 atoms in the ring are believed to be approximately coplanar.^[7]

Despite significant advances in structural biology, it still remains extremely challenging to obtain a GH structure with its natural substrate bound productively.^[8] Consequently, many studies investigating the wild-type reaction have been conducted on mutant enzymes and/or modified substrates.^[5a] To address this limitation, and enable the study of the wild-type enzyme reaction, we used a high-resolution crystal structure of HEWL containing a trisaccharide, 2-acetamido-2-deoxy-D-muramic acid- β (1,4)-2-acetamido-2-deoxy-D-glucose- β (1,4)-2-acetamido-2-deoxy-D-muramic acid (i.e. NAM-B, NAG-C, NAM-D, respectively), situated in the -3, -2, -1 binding sites.^[9] This is the only crystal structure of wild-type HEWL containing a ligand with a NAM subunit occupying the -1 binding site. We re-examined the crystallographic data for two of the HEWL complexes mentioned above (kindly supplied by the original investigators) and created multiple structural models consistent with the crystallographic data (using annealed omit maps^[10] and twin model and multiple conformer refinement^[11], tested by cross-validated R-factor (R_{free})^[12] differing in the conformation of the D site sugar and showing its conformational variability in the complex (see SI: S13). Based on these multiple models, we perform here, extensive conformational sampling by molecular dynamics simulations to explore possible bound structures. We model the reverse reaction (from structures derived from experiment) by QM/MM methods; the choice of modelling the reverse reaction is necessitated by starting with a product complex. Modelling of the reverse of the second step of the forward reaction is in many respects effectively equivalent to the first step of the forward reaction as both involve cleavage of a glycosidic bond assisted by Glu35. Water is a comparable leaving group to the NAG-NAM (E-F sites) disaccharide, with a relatively small basicity difference (1–2 pKa units).^[5b] Here, we apply a significantly higher level of theory (B3LYP-D) than in previous studies,^[5b] allowing accurate characterization of the conformational itinerary adopted by the NAM-D in the -1 binding site, over the course of the reaction. Previous QM/MM simulations applied low levels of theory that do not provide reliable predictions of saccharide ring conformations. Multiple MM MD simulations were performed to generate suitable starting structures for the reaction calculations. QM/MM umbrella sampling calculations were then used to assess the reactivity of the different conformations adopted by the NAM-D when bound in the active site. We compare the reactivity of different conformations and show that substrate distortion is required for efficient reaction.

Crystallographic refinement indicated alternative conformations for the sidechains of Val109 and Asn59, and also suggested four possible conformations of NAM-D. The combination of all these possibilities resulted in sixteen different starting structures for the MD simulations. MM MD calculations were performed with the AMBER12 simulation package,^[13] utilizing the CHARMM22 force-field (with the CMAP correction) for the enzyme and additional sugar parameters which were developed for the trisaccharide based on CHARMM22 sugar parameters,^[14] as applied previously.^[5b] CHAMBER^[15] was used to convert the parameters for use within AMBER. Following equilibration (see SI: S.1), 100ns of MD with periodic boundary conditions was performed on each of the sixteen starting structures. Each

[a] Dr Michael A. L. Limb, Dr Reynier Suardíaz, Dr Ian M. Grant, Prof Adrian J. Mulholland*
School of Chemistry, University of Bristol
Cantock's Close, Bristol, BS81TS (UK)
E-mail: adrian.mulholland@bristol.ac.uk

[b] Present address: Ian M. Grant
Institute of Psychiatry, Psychology & Neuroscience, King's College London
Denmark Hill, London SE5 8AF (UK)
Supporting information for this article is given via a link at the end of the document.)

COMMUNICATION

simulation was repeated five times to ensure significant conformational sampling for the trisaccharide in the active site.

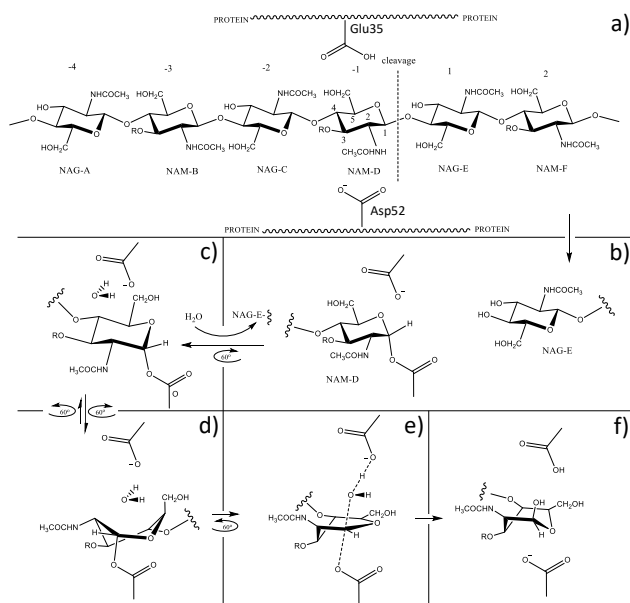


Figure 1. a) Structure of the bound intact substrate. The dashed line indicates the glycosidic bond cleaved in the HEWL-catalysed reaction. b) products of first step of the reaction (i.e. covalent intermediate and hydrolysed saccharide). c) covalent intermediate in the undistorted chair form. d) covalent intermediate in the distorted form. e) transition state of the second step of the reaction (modelled here) and f) product.

Higher level (B3LYP-D) QM/MM 1D and 2D adiabatic mapping calculations were performed using QoMMMA,^[16] with the QM and MM parts of the calculation carried out with Jaguar (version 7.8)^[17] and Tinker (version 6.1).^[18] The QM region (53 atoms) consisted of the NAM-D ring and the sidechains of Glu35 and Asp52, with three hydrogen 'link' atoms. First, 1D adiabatic mapping calculations were performed to simulate the reverse of the second half of the HEWL-catalysed reaction: formation of the covalent intermediate from the trisaccharide product. Second, 2D adiabatic mapping was employed to model the breakdown of the reaction intermediate to give the product, modelling the same step as with 1D, but in the forward direction. The covalent intermediates formed in the 1D calculations were used as the starting structures for the 2D calculations.

QM/MM umbrella sampling MD calculations were performed with AMBER12, using multiple representative structures of the bound conformations of the NAM-D from MM MD calculations. The QM region (the same as in adiabatic mapping calculations) was modelled using the SCC-DFTB method.^[19] All other atoms in the system were treated with the MM force-field as detailed above.

To model the reverse reaction, a single reaction coordinate (RC) was used: $RC1 = d(C1_{NAM-D} - O1_{NAM-D}) - d(C1_{NAM-D} - O\delta2_{Asp52}) / \text{\AA}$. The choice of RC can have profound implications when modelling reactions,^[20] e.g. in glycosidases;^[3a] several RCs were tested, and this was found to be the most suitable to simulate the reaction. Multiple umbrella sampling calculations were performed, scanning from a RC value of -2.2 \AA to 3.6 \AA in 0.1 \AA increments, with 20ps of simulation performed at each window. Additional QM/MM umbrella sampling calculations were performed with 100ps windows to check convergence, (see SI: S.4.3). The RC statistics were printed every 1 fs and the Weighed Histogram Analysis Method (WHAM) was used to construct the free energy profile (FEP) for the reaction.^[21] Potential energy surfaces (PES) were also calculated with higher level (B3LYP-D/6-31+G(d)) QM/MM methods to assess the

reliability of SCC-DFTB for modelling the reaction and conformations.^[22]

Conformational analysis of NAM-D was performed by calculating Cremer-Pople (CP) parameters (See SI: S.2.4).^[23] This enabled the characterization of the exact conformations adopted by NAM-D over the course of the simulations. Determination of whether NAM-D was 'deeply' bound in the active site (and therefore suitably positioned to react) was based on the proximity of the NAM-D to the two catalytic residues in the enzyme: $d(C1_{NAM-D} - O\delta2_{Asp52}) < 4.0 \text{ \AA}$ and $d(O1_{NAM-D} - H\epsilon1_{Glu35}) < 2.0 \text{ \AA}$.

QM/MM and MM MD results concurred in the types of conformations predicted (see SI: S.2, S.3). The results indicate NAM-D was relatively mobile in the trisaccharide complex; consistent with observed crystallographic disorder at the D site. For reaction to occur, the D site ring must be in close proximity to the catalytic residues ('deeply' bound in the -1 site). When 'deeply' bound, the NAM-D adopted $\sim B_{3,0} / E_3$ (distorted) and $\sim ^4C_1$ (undistorted) conformations. Five structures representing each of these two potentially reactive 'deeply' bound states were then used for umbrella sampling calculations. The reverse reaction was modelled (i.e. forming the covalent intermediate from the trisaccharide product).

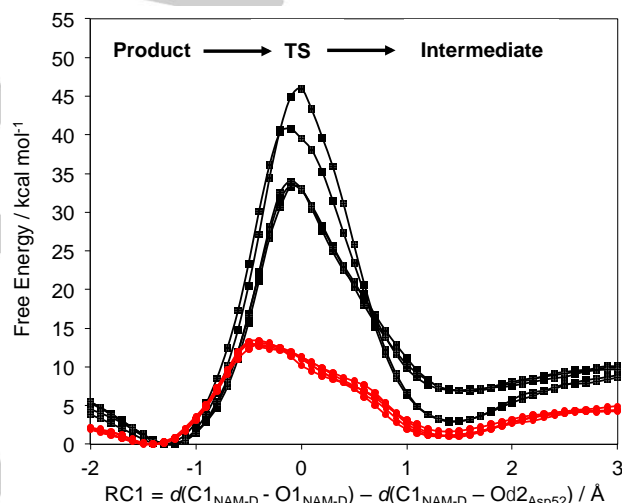


Figure 2. Free energy profiles from SCC-DFTB umbrella sampling of the reverse reaction. Red lines and circles represent the reaction of distorted NAM-D and the black lines and squares are for the reaction of undistorted (chair) NAM-D. Left to right: product, transition state (TS) and covalent intermediate.

The free energy profiles (Fig. 1) show a significantly higher barrier for the reaction of the undistorted conformation. The chair conformations showed average barriers of $37.5 \pm 5.7 \text{ kcal mol}^{-1}$ (\pm standard deviation), significantly higher than the $13.0 \pm 0.2 \text{ kcal mol}^{-1}$ calculated for the distorted conformation. Although the reaction barrier for the undistorted conformation may be overestimated, the difference from that with the distorted conformation ($\sim 25 \text{ kcal mol}^{-1}$) is certainly larger than the likely error of the QM/MM method, and larger than the statistical uncertainty. Only the distorted conformation shows a barrier to reaction consistent with the estimated value of $\sim 17 \text{ kcal mol}^{-1}$ (derived from the experimental measured rate constant for the forward reaction using TS theory).^[24] The larger spread in the reaction barriers for the chair conformation correspond to a larger variation in the undistorted geometries, (see SI: S.3). Note that we do not claim that the calculated barriers for the chair conformation correspond to those for the non-enzymic reaction and thus we do not claim to have calculated the energetic catalytic advantage of distortion; this would require investigation

COMMUNICATION

of the uncatalysed reaction for comparison; this would be most interesting for the forward reaction, which would require an appropriate model of the wild type substrate (not intermediate) complex for comparison. This would be an interesting topic for future work. Also note that the difference in the barriers found here between the distorted and undistorted (chair) conformations is not solely attributable to the conformational energy difference, but also to differences in orientation and stabilizing interactions in the active site.

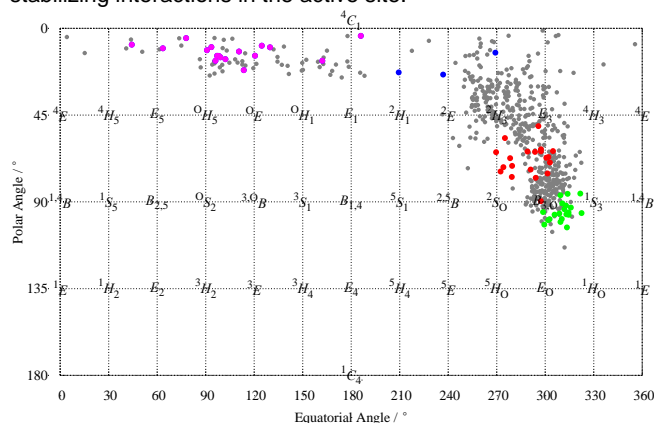


Figure 2. Mercator plot of the distribution of CP parameters of NAM-D for the reaction from a distorted conformation of NAM-D. Green and red points indicate the conformations of the product and TS ensembles, respectively. Blue and purple points indicate the conformations of the intermediate configurations formed with the *anti* and *syn* lone pair of $O\delta 2_{Asp52}$, respectively. Grey points representing the rest of the conformations sampled along the reaction path.

Fig. 2 shows the conformations of the NAM-D ring sampled during reaction from the distorted conformation. The product adopted a $B_{3,O}/E_3$ conformation (historically referred to as a 'sofa').^[9] The transition state (TS) shows $B_{3,O}/E_3$ conformations (with more E_3 character than observed in the product, with a C5-O5-C1-C2 dihedral angle closer to 0°). In all the simulations, the intermediate was found to be covalent ($C1_{NAM-D}-O\delta 2_{Asp52} \sim 1.4$ Å) in agreement with previous studies.^[5] The covalent intermediate showed interesting behaviour, exhibiting either ${}^2S_0/{}^{2,5}B$ or 4C_1 conformations. The simulations indicate that the intermediate conformation is linked to the positioning of the nucleophilic aspartate residue; a novel finding of potentially wide relevance for GHs. Intermediates with a covalent bond formed with the *syn* lone pair of the $O\delta 2_{Asp52}$ atom had an undistorted NAM-D ring, as observed in crystal structures.^[5a] An intermediate formed with the *anti* lone pair had a distorted NAM-D ring. Further MD simulations showed that both types of intermediates could interconvert spontaneously (see SI: S3). These results indicate that the conformational itinerary of the reaction proceeds via *anti* attack, giving rise to a distorted intermediate, which then converts to a more stable *syn*, 4C_1 chair conformation observed experimentally.

QM/MM calculations at a higher level (B3LYP-D/6-31+G(d))/CHARMM27 support the conclusions from the SCC-DFTB QM/MM and MM MD, both in terms of observed conformations and energetics. All three levels of theory predict similar conformations for the product and all the different QM methods concur in the conformations of the intermediate and TS (see SI: S.6). A 2-dimensional PES for the reaction at the B3LYP-D level gave barrier of 13.9 kcal mol⁻¹, similar to the average free energy barrier of 13.0 kcal mol⁻¹. Single point SCS-MP2/aug-cc-pVTZ/MM calculations performed on the B3LYP-D geometries give a barrier of 19.7 kcal mol⁻¹: this indicates both B3LYP and SCC-DFTB underestimate the barrier as is often the case.^[25]

These results clearly indicate that NAM-D must be in a distorted conformation ($\sim B_{3,O}/E_3$) for efficient reaction to occur. While these conclusions are drawn from simulations of the reverse reaction, the same will certainly apply to the forward reaction. Distortion of the product is proposed to give a lower barrier for formation of intermediate for three main reasons: 1. The principle of least nuclear motion,^[26] the distorted conformation requires less nuclear movement to achieve the TS as indicated by the earlier TS in Fig. 1; 2. It enables the repositioning of the axial H1 of NAM-D to a pseudo-equatorial position, allowing the negatively charged Asp52 to effectively stabilize the developing positive charge on the NAM-D in the oxocarbenium ion-like TS; 3. The $C1-O1_{NAM-D}$ bond is positioned pseudo-axially; this satisfies the stereoelectronic preference for an in-line nucleophilic attack on the anomeric centre, allowing population of the σ^* orbital of $C1-O1_{NAM-D}$ bond by the nucleophile (Asp52). Additionally, this geometry positions the $O1_{NAM-D}$ atom on average 0.2 Å closer to Glu35 proton than in the undistorted NAM-D, thus better facilitating its transfer onto the glycosidic oxygen (see SI: S.9).

The results, validated across several levels of theory, are consistent with previous computational and experimental evidence in indicating that a covalent intermediate is formed.^[5] CP analysis of the intermediate suggests that its structure is a distribution of ${}^2S_0/{}^{2,5}B$ and 4C_1 conformations, with a covalent bond formed with either the *anti* and *syn* lone pair of the $O\delta 2_{Asp52}$ respectively. One of the original pieces of evidence against the formation of a covalent intermediate in HEWL was based on the observation that only the *anti* lone pair was suitably orientated to form a covalent bond at $C1_{NAM-D}$.^[9] Results obtained here indicate that formation of the intermediate can in fact take place via attack of either one these lone pairs, with the two forms of the intermediates able to spontaneously interconvert (see SI: S3). This indicates that the current paradigm of an undistorted intermediate formed directly with the *syn* lone pair of the $O\delta 2_{Asp52}$ may not be truly representative of the full catalytic pathway; in fact, an additional conformational step may be involved.

While it has long been postulated that saccharide distortion may be involved in the reaction catalysed by HEWL, direct demonstration of this effect by experiment has proved elusive. QM/MM simulations here demonstrate that distortion of the -1 site NAM sugar (to $\sim B_{3,O}/E_3$) is indeed essential for efficient reaction in lysozyme. Furthermore, these results suggest an intriguing new facet of the conformational itinerary of the reaction, in that it may proceed via a distorted covalent intermediate with a ${}^2S_0/{}^{2,5}B$ conformation, formed by attack of the *anti* lone pair of Asp52, which then converts spontaneously to the undistorted chair conformation (with Asp52 in a *syn* orientation) observed in crystal structures. Altogether, these findings help to resolve long-standing debates on this paradigmatic, textbook enzyme, and suggest conformational details of potentially wide importance for GHs.^[3b, 27]

ASSOCIATED CONTENT

Supporting Information. Full simulation setup details; Cremer-Pople Mercator plots for all QM/MM and MM MD simulations; Geometrical parameters for product, TS and intermediate and corresponding QM regions; B3LYP-D/6-31+G/MM results and analysis; SP calculations. MM MD analysis, NBO analysis and details of crystallographic refinement and structural modelling.

Funding Sources

We thank EPSRC (grant nos. EP/G007705/1, EP/M022609/1 and EP/M013219/1), BBSRC, Pfizer and the SCI (MAAL) for support.

COMMUNICATION

Acknowledgements

We thank Prof. Michael James for most helpfully providing crystallographic data. We thank Prof. Martin Karplus, Prof. Arieh Warshel, Prof. Carol Post, Dr. Carla Mattos and Dr. Dennis Vitkup for useful discussions.

This work was carried out using the computational facilities of the Advanced Computing Research Centre, University of Bristol - <http://www.bristol.ac.uk/acrc/>

Keywords: Enzyme Reaction Mechanisms • QM/MM • Lysozyme • Enzyme Catalysis

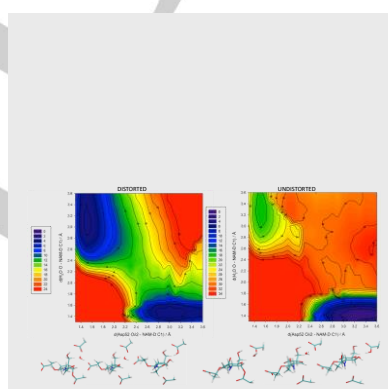
- [1] D. J. Vocadlo, G. J. Davies, *Curr. Opin. Chem. Biol.* **2008**, *12*, 539-555.
 [2] aC. C. F. Blake, D. F. Koenig, G. A. Mair, A. C. T. North, D. C. Phillips, V. R. Sarma, *Nature* **1965**, *206*, 757; bA. Warshel, M. Levitt, *J. Mol. Biol.* **1976**, *103*, 227-249.
 [3] aG. J. Davies, A. Planas, C. Rovira, *Acc. Chem. Res.* **2012**, *45*, 308-316; bG. Speciale, A. J. Thompson, G. J. Davies, S. J. Williams, *Curr. Opin. Struct. Biol.* **2014**, *28*, 1-13; cA. Ardèvol, C. Rovira, *J. Am. Chem. Soc.* **2015**, *137*, 7528-7547.
 [4] G. J. Davies, K. S. Wilson, B. Henrissat, *Biochem. J.* **1997**, *321*, 557-559.
 [5] aD. J. Vocadlo, G. J. Davies, R. Laine, S. G. Withers, *Nature* **2001**, *412*, 835; bA. L. Bowman, I. M. Grant, A. J. Mulholland, *Chem. Commun. (Cambridge, U. K.)* **2008**, 4425-4427.
 [6] D. E. Koshland, *Biological Reviews* **1953**, *28*, 416-436.
 [7] M. L. Sinnott, *Chem. Rev. (Washington, DC, U. S.)* **1990**, *90*, 1171-1202.
 [8] J. D. Gideon, G. W. Stephen, J. V. David, *Aust. J. Chem.* **2009**, *62*, 528-532.
 [9] N. C. J. Strynadka, M. N. G. James, *J. Mol. Biol.* **1991**, *220*, 401-424.
 [10] A. Hodel, S.-H. Kim, A. T. Brünger, *Acta Cryst.* **1992**, *A48*, 851-858.
 [11] aJ. Kuriyan, K. Ōsabay, S. K. Burley, A. T. Brünger, W. A. Hendrickson, M. Karplus, *Proteins* **1991**, *10*, 340-358; bF. T. Burling, A. T. Brünger, *Israel J. Chem.* **1994**, *34*, 165-175.
 [12] aA. T. Brünger, *Meth. Enzymol.* **1997**, *277*, 243-269; bA. T. Brünger, *Nature* **1992**, *355*, 472-475.
 [13] D. A. Case, T. A. Darden, T. E. Cheatham, C. L. Simmerling, J. Wang, R. E. Duke, R. Luo, R. C. Walker, W. Zhang, K. M. Merz, B. Roberts, S. Hayik, A. Roitberg, G. Seabra, J. Swails, A. W. Goetz, I. Kolossváry, K. F. Wong, F. Paesani, J. Vanicek, R. M. Wolf, J. Liu, X. Wu, S. R. Brozell, T. Steinbrecher, H. Gohlke, Q. Cai, X. Ye, J. Wang, M. J. Hsieh, G. Cui, D. R. Roe, D. H. Mathews, M. G. Seetin, R. Salomon-Ferrer, C. Sagui, V. Babin, T. Luchko, S. Gusarov, A. Kovalenko, P. A. Kollman, University of California, San Francisco, **2012**.
 [14] A. D. MacKerell, D. Bashford, M. Bellott, R. L. Dunbrack, J. D. Evanseck, M. J. Field, S. Fischer, J. Gao, H. Guo, S. Ha, D. Joseph-McCarthy, L. Kuchnir, K. Kuczera, F. T. K. Lau, C. Mattos, S. Michnick, T. Ngo, D. T. Nguyen, B. Prodhom, W. E. Reiher, B. Roux, M. Schlenkrich, J. C. Smith, R. Stote, J. Straub, M. Watanabe, J. Wiórkiewicz-Kuczera, D. Yin, M. Karplus, *The Journal of Physical Chemistry B* **1998**, *102*, 3586-3616.
 [15] M. F. Crowley, M. J. Williamson, R. C. Walker, *Int. J. Quantum Chem.* **2009**, *109*, 3767-3772.
 [16] aR. Lonsdale, J. N. Harvey, A. J. Mulholland, *Chem. Soc. Rev.* **2012**, *41*, 3025-3038; bR. Lonsdale, K. T. Houghton, J. Žurek, C. M. Bathelt, N. Foloppe, M. J. de Groot, J. N. Harvey, A. J. Mulholland, *J. Am. Chem. Soc.* **2013**, *135*, 8001-8015.
 [17] A. D. Bochevarov, E. Harder, T. F. Hughes, J. R. Greenwood, D. A. Braden, D. M. Philipp, D. Rinaldo, M. D. Halls, J. Zhang, R. A. Friesner, **2013**, *113*, 2110-2142.
 [18] J. W. Ponder, F. M. Richards, *J. Comput. Chem.* **1987**, *8*, 1016-1024.
 [19] T. Frauenheim, G. Seifert, M. Elsterner, Z. Hajnal, G. Jungnickel, D. Porezag, S. Suhai, R. Scholz, *phys. stat. sol. (b)* **2000**, *217*, 41-62.
 [20] P. G. Bolhuis, D. Chandler, C. Dellago, P. L. Geissler, *Annu. Rev. Phys. Chem.* **2002**, *53*, 291-318.
 [21] A. Grossfield, *WHAM: the weighted histogram analysis method*, version 2.0.9, <http://membrane.urmc.rochester.edu/content/wham> **2013**.
 [22] G. Stefan, *J. Comput. Chem.* **2006**, *27*, 1787-1799.
 [23] aD. Cremer, J. A. Pople, *J. Am. Chem. Soc.* **1975**, *97*, 1354-1358; bA. Berces, D. M. Whitfield, T. Nukada, *Tetrahedron* **2001**, *57*, 477-491.
 [24] D. M. Chipman, *Biochemistry* **1971**, *10*, 1714-1722.
 [25] aR. Suardíaz, P. G. Jambrina, L. Masgrau, À. González-Lafont, E. Rosta, J. M. Lluch, *J. Chem. Theory Comput.* **2016**, *12*, 2079-2090; bF. Claeysens, J. N. Harvey, F. R. Manby, R. A. Mata, A. J. Mulholland, K. E. Ranaghan, M. Schütz, S. Thiel, W. Thiel, H.-J. Werner, **2006**, *45*, 6856-6859; cI. Y. Zhang, J. Wu, X. Xu, *Chem. Commun. (Cambridge, U. K.)* **2010**, *46*, 3057-3070.
 [26] J. Hine, in *Adv. Phys. Org. Chem., Vol. 15* (Eds.: V. Gold, D. Bethel), Academic Press, **1977**, pp. 1-61.
 [27] aGideon J. Davies, Spencer J. Williams, **2016**, *44*, 79-87; bA. Ardèvol, J. Iglesias-Fernández, V. Rojas-Cervellera, C. Rovira, **2016**, *44*, 51-60.

Entry for the Table of Contents (Please choose one layout)

Layout 1:

COMMUNICATION

QM/MM calculations on lysozyme show significant distortion of the bound saccharide is required to facilitate the catalytic reaction. TOC shows the 2D PES from undistorted (left) and distorted (right) intermediate. The results indicate that reaction occurs via anti attack of Asp52, with subsequent conformational change.



Michael A. L. Limb, Reynier Suardíaz,
Ian M. Grant, Adrian J. Mulholland*

Page No. – Page No.

Title

QM/MM Simulations Show Saccharide
Distortion is Required for Reaction in
Hen Egg-White Lysozyme